Arch. Metall. Mater. **63** (2018), 2, 673-680

DOI: 10.24425/122393

Y. LIU *,**#, X. WANG***, Y. SUN**, F. DU***, Y. GAO*, F. WANG*, J. WANG*

A VISUAL DETECTION METHOD OF LONGITUDINAL CRACK BASED ON COMPUTER IMAGE PROCESSING DURING SLAB CONTINUOUS CASTING

Based on the mould temperature measured by thermocouples during slab continuous casting, a difference of temperature thermograph is developed to detect slab cracks. In order to detect abnormal temperature region caused by longitudinal crack, the suspicious regions are extracted and divided by virtue of computer image processing algorithms, such as threshold segmentation, connected region judgement and boundary tracing. The abnormal regions are then determined and labeled with the eight connected component labeling algorithm. The boundary of abnormal region is also extracted to depict characteristics of longitudinal crack. Based on above researches, longitudinal crack with abnormal temperature region can be detected and is different from other abnormalities. Four samples of temperature drop are picked up to compare with longitudinal crack on the abnormal region formation, length, width, shape, et al. The results show that the abnormal region caused by longitudinal crack has a linear and vertical shape. The height of abnormal region is more than the width obviously. The ratio of height to width is usually larger than that of other temperature drop regions. This method provides a visual and easy way to detect longitudinal crack and other abnormities. Meanwhile it has a positive meaning to the intelligent and visual mould monitoring system of continuous casting.

Keywords: longitudinal crack; visual detection; image processing; continuous casting

1. Introduction

The crack on the strand surface is a very non-desired incident during slab continuous casting. These defects may decrease steel product quality and cause high cost, wherein longitudinal crack is the most serious one [1]. Sometimes, a large longitudinal crack will cause a more serious breakout accident. Even though a small crack arises on the slab surface, finishing treatment is also needed for subsequent steel rolling [2,3]. Based on former researches, slab cracks are influenced by metallurgical factors and thermal stress [4-6]. Slab cracks generally form at the meniscus and are influenced by the physical and chemical property of mould powder, especially for peritectic steel with the large shrinkage [7,8]. A proper mould powder is helpful to enhance slab quality and decrease cracks [9-11]. Adjustment of the heat extraction at the meniscus can also improve slab quality, such as changing copper plate thickness, mould coating thickness/conductivity, cooling water velocity, cooling channel configuration and mould flux composition [12,13]. These researches provide basis to improve continuous casting process and operation, which is helpful to reduce the occurrence of slab cracks.

However, the surface cracks cannot be avoided due to the complicated steel grade, mould powder and actual operation. The crack detection or prediction methods need to be studied. Mould thermograph monitoring has been studied and used more and more in recent years, such as sticker breakout detection, SEN hole detection, abnormality of mould powder detection [14-16]. Thomas used a finite-element model to simulate thermo-mechanical behavior of the solidifying shell in the thin-slab caster mould [17]. Schwerdtfeger proposed a method to predict surface crack formation in continuous casting, based on reduction of area functions measured by the tensile test [2]. Tirian built up a neural network for crack prediction to improve the steel-casting process performance [18]. Xu proposed a novel detection method of slab longitudinal surface crack with optical technology [19]. Nevertheless, detection of slab cracks is immature due to the invisible mould and complicated continuous casting process. These cracks are still observed by worker's naked eyes in production. A quick and early detection method is important to continuous casting monitoring. If cracks can be detected in the mould, the operator can adjust continuous casting process timely to avoid continuous waste. The slab quality could be improved too. Therefore, detection method of slab cracks needs to be studied further more.

In this work, based on the measured temperature signals from the mould monitoring system, a temperature thermograph is constructed to detect the longitudinal crack visually via a determination of the difference of temperature. The formation

* NORTHEAST ELECTRIC POWER UNIVERSITY, SCHOOL OF MECHANICAL ENGINEERING NO. 169 CHANGCHUN ROAD, CHUANYING DISTRICT, JILIN, CN 132012
** DALIAN UNIVERSITY OF TECHNOLOGY, SCHOOL OF INFORMATION AND COMMUNICATION ENGINEERING, NO.2 LINGGONG ROAD, GANJINGZI DISTRICT, DALIAN, CN 116024
*** DALIAN UNIVERSITY OF TECHNOLOGY, SCHOOL OF MATERIALS SCIENCE AND ENGINEERING, NO.2 LINGGONG ROAD, GANJINGZI DISTRICT, DALIAN, CN 116024
# Corresponding author: greatliudy123@163.com

and movement of longitudinal crack in the thermograph are captured by virtue of the computer image processing algorithms. The abnormal regions are divided from the normal regions with segmentation algorithm. The edge of longitudinal crack can be detected with 8-connected and boundary tracing algorithm. Based on above process, the characteristics of longitudinal crack are compared to steady production and other abnormalities, such as casting speed down, abnormal fluctuation, nonuniform distribution of mould slag. The results show that longitudinal crack has obvious characteristics from others. This study provides a new and visual detection method of longitudinal crack in mould, especially thermocouple arrangement with large density, which can help operator to find out cracks early.

2. Mould temperature visualization

2.1. Experimental basis

This paper is based on an arc continuous caster, the radius of which is 10.75 m and the metallurgical length is 28.8 m. The slab width is from 1.8 to 2.7 m, the thickness is between 0.22 and 0.32 m, and the slabs are cast at maximum casting speeds of 1.2 and 0.75 m/min, respectively. In order to detect the formation and development of slab surface cracks, the mould copper plates contain many thermocouples: the wide face has 19 columns of thermocouples with 0.15 m spacing, whereas the narrow face has one column of thermocouples. Three rows of thermocouples are located, respectively, 0.21, 0.325 and 0.445 m below the mould top. The total number of embedded thermocouples is 120. The mould length is 0.9 m and the operational mould level is 0.1m from the top of the mould. A schematic diagram of the thermocouple arrangement and the installation is shown in Fig. 1.

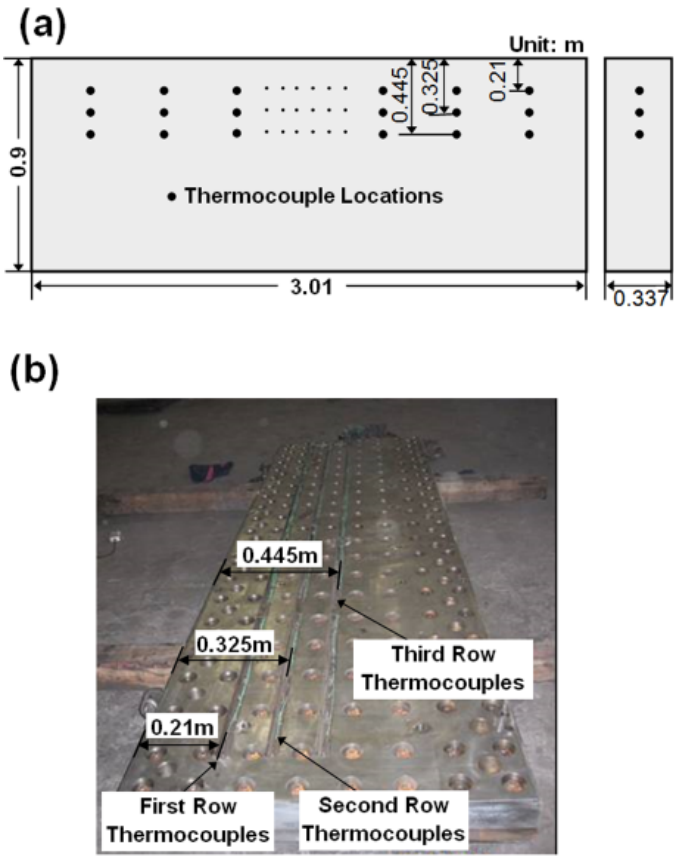

Fig. 1. Schematic diagram of the thermocouple arrangement (a) and real installation (b)

2.2. Temperature visualization

The temperature readings from mould thermocouples are collected and updated per second by the monitoring system, and stored in a matrix. In order to get the temperatures of the whole copper plates, the outside radius, right-narrow, inside radius and left-narrow faces will be rearranged along the clockwise direction, as shown in Fig. 2. Coordinate x is the horizontal direction and y is the casting direction. The unknown temperatures between the thermocouples are calculated by the interpolation algorithm according to the known thermocouple temperatures and stored in the matrix $[W_b \times H]$ and $[W_n \times H]$, where W_b and W_n are the number of the pixels on the wide and narrow face, respectively. H is the number of pixels in casting direction. It is important to note that the pixels are according to certain area on the copper plates. Of course, an area of region can be calculated by pixel number. There is a corresponding interrelationship between the temperature value and pixel color, and the mould temperature thermograph has been built up with the computer graphics, as shown in Fig. 2. The thermograph shows the temperature values and distribution on the mould copper plates at any time. In the Fig. 2, it has a symmetrical and uniform temperature which reflects the virtual condition in mould. If some abnormalities arise in mould, such as the abnormalities of the flow field, submerged entry nozzle and powder consumption status, they can be detected by this thermograph too. And it can be also used as fundamental data to predict longitudinal crack.

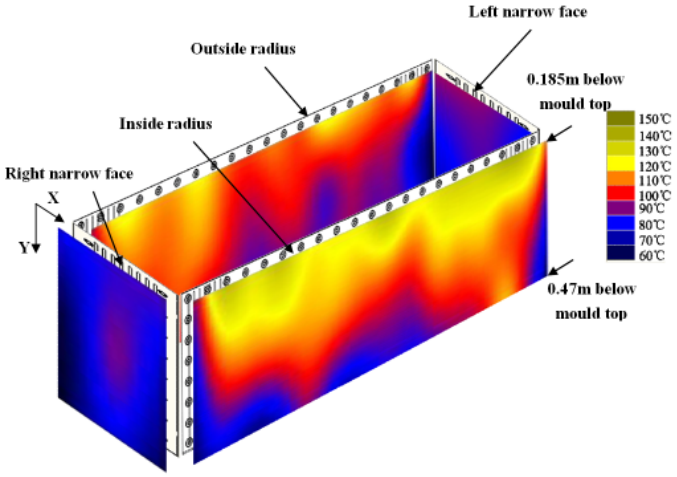

Fig. 2. The visualization of temperature field for four mould copper plates

2.3. Difference of temperature visualization

Thermograph can show mould temperature and its distribution for operator at preset. Sometimes operator also would like to inspect difference of temperature compared with historical temperatures in order to find out some abnormalities. However, in temperature thermograph as shown in Fig. 2, the historical temperatures cannot be got. Therefore the present difference of temperature $D_0[x,y]$ is computed with Eq. (1). The present $D_0[x,y]$ is a relative value that present temperature $T_0[x,y]$ subtracts average temperature $T_a[x,y]$. The average temperature $T_a[x,y]$ is computed with Eq. (2).

$$D_0[x,y] = T_0[x,y] - T_a[x,y] \tag{1}$$

$$T_a[x,y] = \frac{T_1[x,y] + T_2[x,y] + \ldots + T_n[x,y]}{n} \tag{2}$$

where, $T_a[x,y]$ is an average temperature value of pixel point $[x,y]$ in mould thermograph. The mould temperature at present is lower than historical temperatures if $D_0[x,y]$ is less than 0. If the casting speed is not decreased at this time, there may be a longitudinal crack on strand surface in mould. The operator should pay more attention on this abnormal region. The mould temperature at present is higher than historical temperatures if $D_0[x,y]$ is more than 0. There may be a breakout happened in mould. The mould temperature at present is equal to historical temperatures if $D_0[x,y]$ is 0. It shows that the mould temperature is normal. If there is an abnormal region, abnormal characteristics can be extracted further for analysis.

The difference of temperature $D_0[x,y]$ shows temperature variation below meniscus, which is stored in matrix $[W_b \times H]$ and $[W_n \times H]$ in chronological order. H is the number of pixels vertically. Based on above data, a corresponding relationship between difference of temperature and mould pixel point can be built up. By virtue of computer image and OpenGL technology, difference of temperature on mould copper plate will be shown on two-dimensional graph. The thermograph with temperature and difference of temperature is show in Fig. 3.

Figure 3a is a temperature thermograph during normal casting state. Figure 3b is a temperature thermograph with a longitudinal surface crack, as shown "Temperature falling region". Although there is a temperature falling region in Fig. 3b, if it is not compared to Fig. 3a, this cold region is hardly to be found. However, this cold region is more obvious in the new difference of temperature thermograph, as shown in Fig. 3c. A longitudinal crack may arise on slab surface concluded from this cold region.

3. Capture abnormal regions with image processing

3.1. Region segmentation

Non-uniform slag film and mould level fluctuation are two reasons of temperature variation on mould copper plates, and create problems to detect and recognize longitudinal cracks. In order to distinguish normal temperature variation from LFC (longitudinal surface crack) temperature, difference of temperature lower than –3.5°C is considered to be abnormal. Thus, the abnormal temperature regions were extracted with the threshold segmentation algorithm, which is convenient to confirm the LFC regions furthermore. The threshold algorithm takes the form as Eq. (3).

$$b(x,y) = \begin{cases} 1, & D_0(x,y) \le Z \\ 0, & D_0(x,y) > Z \end{cases} \tag{3}$$

where, $D_0(x,y)$ is the difference of temperature at the pixel position (x,y); $b(x,y)$ is the binary expression of the thermograph,

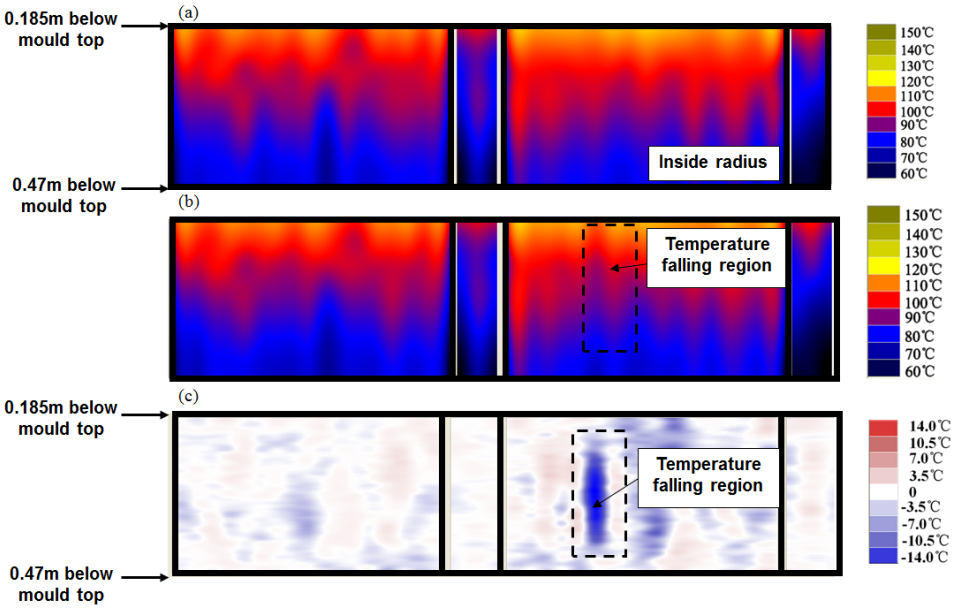

Fig. 3. Temperature thermograph and difference of temperature thermograph of mould copper plates (a) temperature thermograph on steady state; (b) temperature thermograph at T moment; (c) difference of temperature thermograph at T moment

and its value is 0 or 1; If difference of temperature $D_0(x,y)$ is larger than threshold Z, the $b(x,y)$ value is 0, otherwise the value is 1 and the corresponding pixel is considered to be abnormal; Coordinates x and y mean, respectively the horizontal and casting direction.

3.2. Connected region and labeling algorithm

In the thermograph, the relationship between the center pixel and the neighbors can be depicted as the form of 4-connected and 8-connected. In Fig. 4a, if the value of the center pixel is the same as the top, down, left and right, the center pixel is considered to be connected with the four neighbors. While the 8-connected includes the 4-connected and other four directions, such as lower left, lower right, upper left and upper right, as shown in Fig. 4b. The pixels in the thermograph may be connected to one or more pixels after threshold segmentation. The region's shape, area, position and boundary are determined by the connected region algorithm. The 8-connected algorithm is more accurate than 4-connected algorithm, which can depict longitudinal crack characteristics better. Thus, the 8-connected is adopted in this paper.

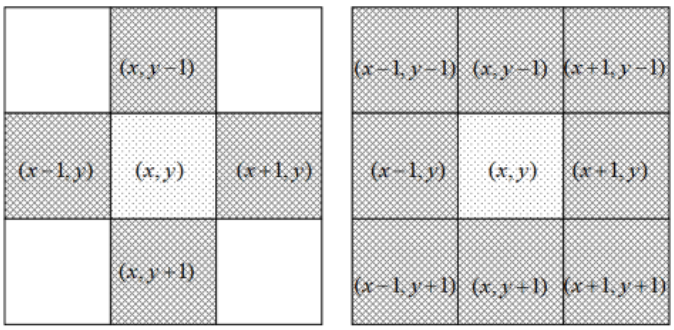

(a) (b)

Fig. 4. Interrelationship between center pixel and neighbours (a) 4-connected; (b) 8-connected

The pixels in the thermograph can be divided into different regions using 8-connected algorithm, and marked with the corresponding labels. This is called labelling algorithm. Every pixel in the image matrix $b(x,y)$ would be scanned point-by-point from the left to right and the top to down, and the region labels were distributed with the Eqs. (4-6).

if $b(x,y) = 0$

$$t(x,y) = 0 \tag{4}$$

if $b(x,y) = 1$ and $b(x-i, y-j) = 1$

$$t(x,y) = t(x-i, y-j) \tag{5}$$

if $b(x,y) = 1$ and $b(x-i, y-j) = 0$

$$t(x,y) = m, (m = m + 1) \tag{6}$$

where, $\{i, j \in M_s\}$. The labels are saved in matrix $t(x,y)$, such as 0,1,2,3…… in Fig. 5; M_s is a matrix to save four directions around the centre pixel, including the upper right $b(x+1, y-1)$, the top $b(x, y-1)$, the upper left $b(x-1, y-1)$ and the left $b(x-1, y)$, and those directions have a descending priority; the natural number m is a maximum label at present.

After scanning the pixels in the thermograph, the abnormal temperature regions are confirmed. As shown in Fig. 5, the region of label 0 has a normal difference of temperature, and is called the background, whereas the regions of labels 1, 2 and 3 are abnormalities. It can be seen that the abnormal region of label 1 has the largest area, linear shape and vertical direction characteristics. The abnormal regions of label 2 and 3 with a small area may be some defects or disturbances.

3.3. Boundary tracing

Boundary is a primary feature, which can show shape and direction of abnormal regions. Abnormal region edge of longitudinal crack can be extracted with boundary tracing algorithm. The principal is as follow: the abnormal region is scanned point

R \ C	0	1	2	3	4	5	6	7	8	9	10	11	12	13	14	15
0	0	0	0	0	1	0	0	0	0	0	0	0	0	0	0	0
1	0	0	0	0	1	1	0	0	0	0	0	0	2	0	0	0
2	0	0	0	0	1	1	0	0	0	0	0	0	2	0	0	0
3	0	0	0	0	1	1	0	0	0	0	0	0	2	0	0	0
4	0	0	0	0	1	1	0	0	0	0	0	2	2	2	0	0
5	0	0	0	0	1	1	0	0	0	0	0	0	2	0	0	0
6	0	0	0	0	1	1	0	0	0	0	0	0	2	0	0	0
7	0	0	0	0	1	1	0	0	0	0	0	0	0	0	0	0
8	0	0	0	0	1	1	0	0	0	0	0	0	0	0	0	0
9	0	0	0	0	1	1	0	0	0	0	0	0		0	0	0
10	0	0	0	0	1	1	0	0	0	0	0	0	3	0	0	0
11	0	0	0	0	1	1	0	0	0	0	0	3	3	3	3	0
12	0	0	0	0	1	1	0	0	0	0	0	3	3	3	3	0
13	0	0	0	0	1	1	0	0	0	0	0	0	3	0	0	0
14	0	0	0	0	1	0	0	0	0	0	0	0	0	0	0	0
15	0	0	0	0	0	0	0	0	0	0	0	0	0	0	0	0

Fig. 5. A schematic diagram of labeling result for the connected regions

by point from the bottom left corner to the top right corner in the thermograph. The first abnormal pixel of the connected region is set as the started point of edge. For example, as shown in Fig. 6, $t(x,y)$ is a started point of edge. If the top left point $t(x-1, y-1)$ is a point with the same region label, $t(x-1, y-1)$ is also a boundary point. Then $t(x-1, y-1)$ is set to be a new started point and this direction is rotated 90° anticlockwise as a new one. The boundary point continues to be detected in this new direction. If the top left point $t(x-1, y-1)$ is not a point with the same region label and this direction is rotated 45° clockwise until a new point is found. When a new boundary point is found, the direction rotates 90° anticlockwise as a new one and continues to search next boundary point. This loop will be end until back to the start point.

4. Experimental result

Four samples of temperature falling are selected from 6875 casting heat numbers as shown in Fig. 7. In Fig. 7a$_1$, some abnormal regions of temperature falling arises in difference of temperature thermograph at 14:31:44. Then these regions connect to each other after 43 seconds and become to be a larger temperature falling region. This is the basic temperature characteristics caused by casting speed down, such as changing submerged entry nozzle. Thus, a region of temperature falling with large area arises in difference of temperature thermograph when casting speed is down. In Fig. 7b$_1$, there are some small and scattered regions of temperature falling with different shape, which reflects some temperature fluctuations randomly in mould.

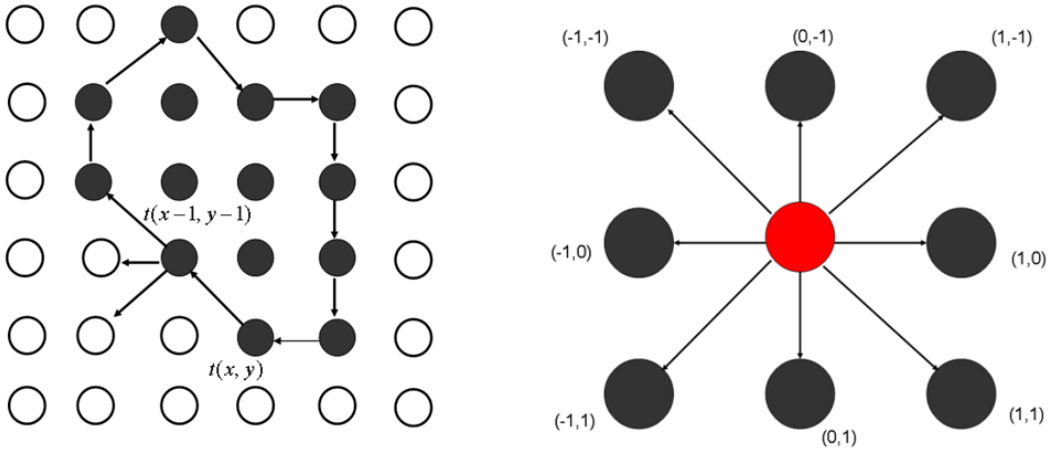

Fig. 6. Schematic diagram of boundary tracing (a) boundary tracing process (b) eight numbers and offset of the center pixel

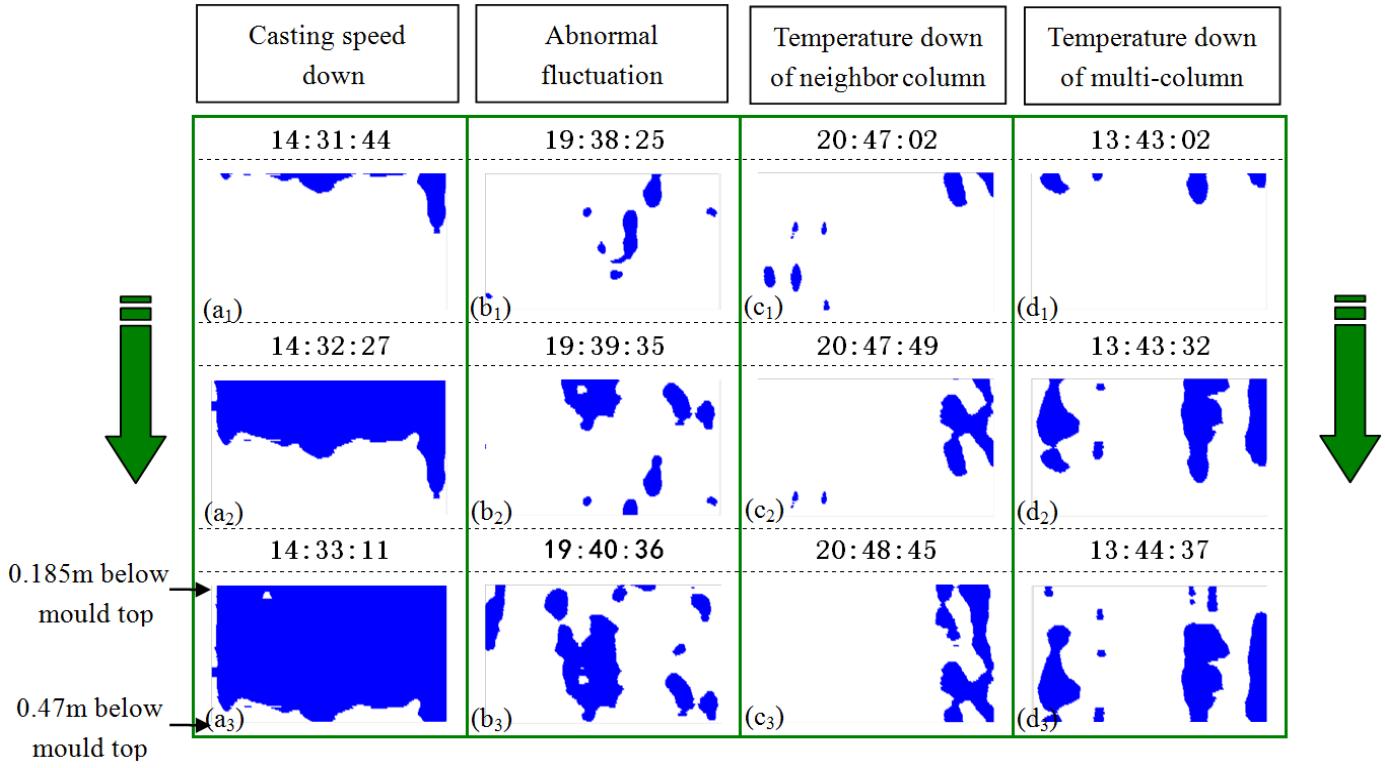

Fig. 7. Abnormal regions of four temperature falling samples

This unsteady heat transfer may be caused by the nonuniform mould slag or even nonuniform strand shell, which decreases slab quality to some extent. Thus the operator should pay more attention to homogeneity of mould flux in production. In Fig. 7c and 7d series, some cold regions of temperature falling arise around the mould copper plate corners. In Fig. 7c series, these regions are neighbor columns, while Fig. 7d has 4 columns at least. The mould copper corner is prone to form cracks or longitudinal crack. If the mould copper corner has cold regions continuously, these locations may have some abnormalities, even serious cracks. The operator should inspect the hot strand out of mould in order to confirm the defects.

Figure 8 shows difference of temperature thermographs at t_1, t_2 and t_3. Time t_1, t_2 and t_3 are three continuous moments to show formation and move of cold regions. Based on above algorithms, regions of temperature falling are segmented and extracted. It can be seen that the number of cold regions is not very much in Figure 8. It means that the whole casting process is normal and steady. The mould flux and casting parameters are suitable and helpful to product high quality slab. But a cold region arises at the top of the thermograph around center line of mould at t_1. This is the beginning of longitudinal surface crack. Then this cold region becomes to be a larger one after 29 seconds as shown in Fig. 8b. Over time, the whole cold region c appears after 22 seconds in Fig. 8c, which has the largest area. The cold region a, b and c look like as a vertical line. The height is more than width obviously and the ratio of height to width is usually larger than those of other regions. Therefore this is a primary characteristic of longitudinal surface crack. The boundaries are also extracted and changed to red color as shown in Fig. 8c. All above characteristics of temperature falling region are clearly different to those in Fig. 7. All above characteristics detected by thermograph are accord with those in Fig. 9 which is a real longitudinal crack in actual production. The results show that this thermograph can capture the main characteristics of longitudinal surface crack, especially length, width and ratio of length to width. These visual characteristics can be convenient for operators and on-line recognition or prediction of longitudinal surface crack.

5. Conclusion

Based on the on-line mould temperature monitoring system for continuous casting slab, a difference of temperature thermograph is developed to detect longitudinal crack with the advantage of computer vision technology. Based on above methods, the abnormal regions detected by thermograph are segmented and extracted with the image processing algorithms. And the longitudinal crack characteristics are also compared with four samples of temperature falling selected from 6875 casting heat numbers. The large areas of temperature falling regions are the obvious characteristic of casting speed down in thermograph, such as changing submerged entry nozzle. When the cold regions of temperature falling are near corner, the operators should pay more attention to the possible cracks. Meanwhile, this thermograph can capture the linear and vertical shape of longitudinal crack easily. The region height of temperature falling is more

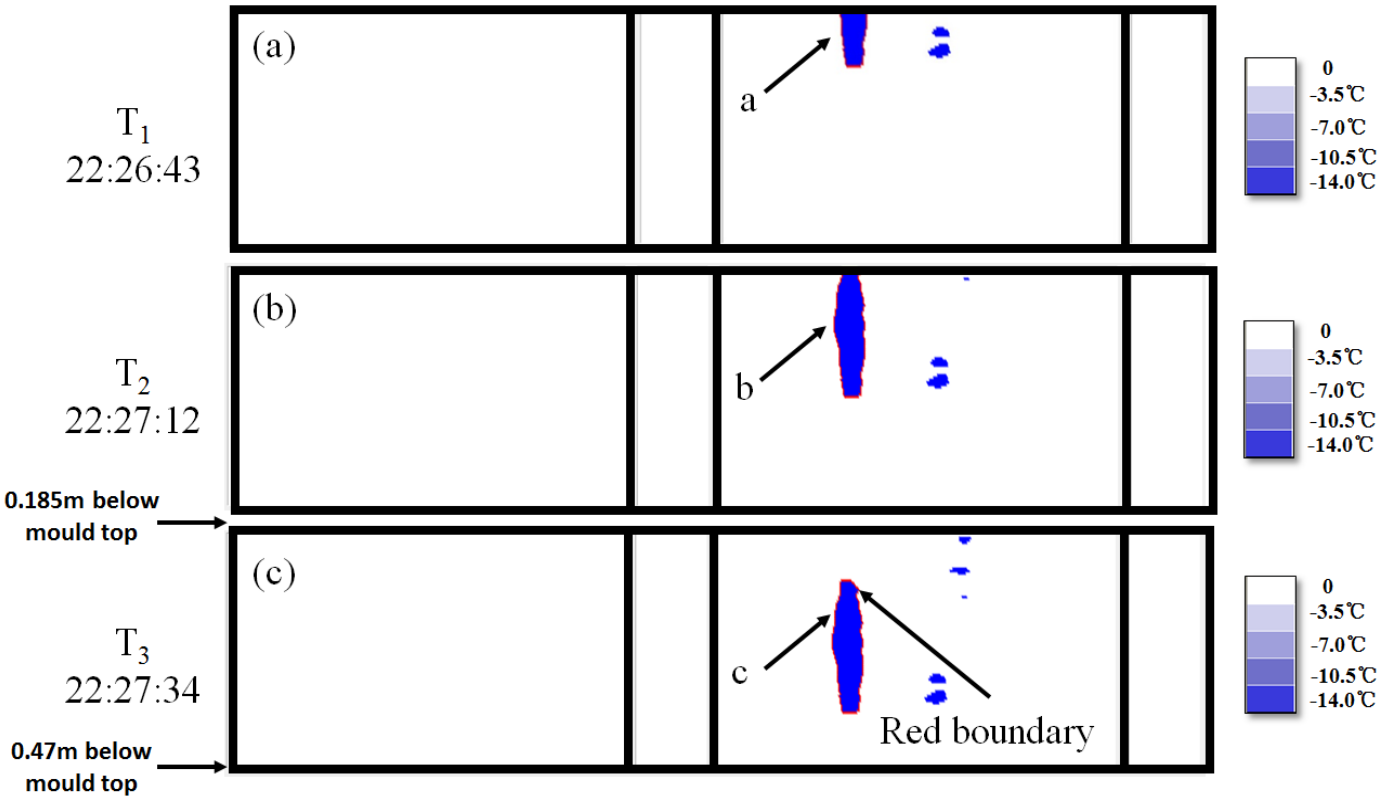

Fig. 8. A longitudinal crack in difference of temperature thermograph (a) t_1 moment; (b) t_2 moment; (c) t_3 moment

Fig. 9. A longitudinal surface crack on inside radius

than the width obviously. The ratio of height to width of cold region caused by longitudinal crack is usually larger than those of cold regions. The direction of longitudinal crack region is almost parallel to casting direction. This visual method provides a visual and easier method to detect longitudinal crack, which is helpful to found longitudinal crack. It also can promote the intelligence and visualization of the mould temperature monitoring system.

Acknowledgements

We would like to acknowledge financial support from the National Natural Science Foundation of China (51704073/51004012/51505077), Science and Technology Development of Jilin Province (20180520065JH /20170520099JH), "13th Five-Year Plan" Science and Technology Research Project of Jilin Provincial Education Department (JJKH20180419KJ), and Technology Innovation Development Project of Jilin City (20166013). This project was also given financial support by the China Postdoctoral Science Foundation (2013T60511/2017M611209), the Fundamental Research Funds for the Central Universities (3132017009), Natural Science Foundation of Liaoning Province (20170540083), and Key Laboratory of Solidification Control and Digital Preparation Technology (Liaoning Province).

REFERENCES

[1] J. Konishi, M. Militzer, I.V. Samarasekera, J.K. Brimacombe, Modeling the formation of longitudinal facial cracks during continuous casting of hypoperitectic steel, Metallurgical and Materials Transactions B **33**, 413-423 (2002).

[2] K. Schwerdtfeger, K.H. Spitzer, Application of reduction of area--temperature diagrams to the prediction of surface crack formation in continuous casting of steel, ISIJ International **49**, 512-520 (2009).

[3] O.B. Isaev, V.V. Emelyanov, V.V. Kislitsa, Y.I. Matrosov, L.S. Lepikhov, Effect of the carbon content of low-alloy steels on the surface quality of continuous-cast semifinished products and rolled plates, Metallurgist **48**, 210-213 (2004).

[4] B. Hadala, A. Cebo-Rudnicka, Z. Malinowski, A. Goldasz, The influence of thermal stress and strand bending on surface defects formation in continuous cast strands, Archives of Metallurgy and Materials **56**, 367-377 (2011).

[5] H.L. Yu, X.H. Liu, Longitudinal crack on slab surface at straightening stage during continuous casting using finite element method, Journal of Central South University of Technology **17**, 235-238 (2010).

[6] J.K. Park, I.V. Samarasekera, B.G. Thomas, U.S. Yoon, Thermal and mechanical behavior of copper molds during thin-slab casting

(II): Mold crack formation, Metallurgical and Materials Transactions B **33**, 437-449 (2002).

[7] Y. Kanbe, T. Ishii, H. Todoroki, K. Mizuno, Prevention of longitudinal cracks in a continuously cast slab of Fe-Cr-Ni superalloy containing Al and Ti, International Journal of Cast Metals Research **22**, 143-146 (2009).

[8] J.K. Brimacombe, K. Sorimachi, Crack formation in the continuous casting of steel, Metallurgical Transactions B **8**, 489-505 (1977).

[9] M. Kawamoto, Y. Tsukaguchi, N. Nishida, T. Kanazawa, S. Hiraki, Improvement of the initial stage of solidification by using mild cooling mold powder, ISIJ International **37**, 134-139 (1997).

[10] S. Sridhar, K.C. Mills, S.T. Mallaband, Powder consumption and melting rates of continuous casting fluxes, Ironmaking & Steelmaking **29**, 194-198 (2002).

[11] X. Yu, G.H. Wen, P. Tang, H. Wang, Investigation on viscosity of mould fluxes during continuous casting of aluminium containing TRIP steels, Ironmaking & Steelmaking **36**, 623-630 (2009).

[12] R.B. Mahapatra, J.K. Brimacombe, I.V. Samarasekera, Mould behavior and its influence on quality in the continuous casting of steel slabs: Part II. Mould heat transfer, Mould heat transfer, Mould Flux Behavior, Formation of Oscillation Marks, Longitudinal off-corner depressions, and subsurface cracks, Metallurgical Transactions B **22**, 875-888 (1991).

[13] L. Zhang, G.D. Xu, X.H. Wang, Z.Y. Zhu, Investigation on Longitudianal surface cracks of CC slabs for container, Iron and Steel **37**, 19-25 (2002).

[14] J. Watzinger, A. Pesek, N. Huebner, M. Pillwax, O. Lang, MoldExpert-operational experience and future development, Ironmaking & Steelmaking **32**, 208-212 (2005).

[15] F. He, D.F. He, A.J. Xu, H.B. Wang, N.Y. Tian, S. Chang, G. Bu, A method for plotting the on-line thermal map of a continuous casting mould, Journal of University of Science and Technology Beijing **36**, 952-958 (2014).

[16] Y.Y. Zhai, Z.G. Ao, Thermal imaging analysis of the prediction of breakout in continuous casting, Control Engineer of China **22**, 1251-1254 (2015).

[17] L.C. Hibbeler, B.G. Thomas, B. Santillana, A. Hamoen, A. Kamperman, Longitudinal face crack prediction with thermo-mechanical models of thin slabs in funnel moulds, Metall. Ital. **6**, 1-10 (2009).

[18] G.O. Tirian, I. Filip, G. Prostean, Adaptive control system for continuous steel casting based on neural networks and fuzzy logic, Neurocomputing **125**, 236-245 (2014).

[19] K. Xu, C.L. Yang, P. Zhou, C. Yang, X.G. Li, On-line detection technique of surface cracks for continuous casting slabs based on linear lasers, Journal of University of Science and Technology Beijing **32**, 1620-1624 (2009).